ARTICLE

Bi-allelic *GOT2* Mutations Cause a Treatable Malate-Aspartate Shuttle-Related Encephalopathy

Clara D.M. van Karnebeek,[1,2,3,19,21,*] Rúben J. Ramos,[3,4,21] Xiao-Yan Wen,[5,6,21] Maja Tarailo-Graovac,[7,8,21] Joseph G. Gleeson,[9] Cristina Skrypnyk,[10] Koroboshka Brand-Arzamendi,[5] Farhad Karbassi,[5] Mahmoud Y. Issa,[11] Robin van der Lee,[12] Britt I. Drögemöller,[13,14] Janet Koster,[15] Justine Rousseau,[16] Philippe M. Campeau,[16] Youdong Wang,[5] Feng Cao,[17] Meng Li,[5] Jos Ruiter,[15] Jolita Ciapaite,[3,4] Leo A.J. Kluijtmans,[3,18] Michel A.A.P. Willemsen,[3,19] Judith J. Jans,[3,4] Colin J. Ross,[13] Liesbeth T. Wintjes,[3,18,20] Richard J. Rodenburg,[3,18,19,20] Marleen C.D.G. Huigen,[3,18] Zhengping Jia,[17] Hans R. Waterham,[3,15] Wyeth W. Wasserman,[12] Ronald J.A. Wanders,[3,15] Nanda M. Verhoeven-Duif,[3,4] Maha S. Zaki,[11] and Ron A. Wevers[3,18,*]

Early-infantile encephalopathies with epilepsy are devastating conditions mandating an accurate diagnosis to guide proper management. Whole-exome sequencing was used to investigate the disease etiology in four children from independent families with intellectual disability and epilepsy, revealing bi-allelic *GOT2* mutations. In-depth metabolic studies in individual 1 showed low plasma serine, hypercitrullinemia, hyperlactatemia, and hyperammonemia. The epilepsy was serine and pyridoxine responsive. Functional consequences of observed mutations were tested by measuring enzyme activity and by cell and animal models. Zebrafish and mouse models were used to validate brain developmental and functional defects and to test therapeutic strategies. *GOT2* encodes the mitochondrial glutamate oxaloacetate transaminase. GOT2 enzyme activity was deficient in fibroblasts with bi-allelic mutations. GOT2, a member of the malate-aspartate shuttle, plays an essential role in the intracellular NAD(H) redox balance. *De novo* serine biosynthesis was impaired in fibroblasts with *GOT2* mutations and GOT2-knockout HEK293 cells. Correcting the highly oxidized cytosolic NAD-redox state by pyruvate supplementation restored serine biosynthesis in GOT2-deficient cells. Knockdown of *got2a* in zebrafish resulted in a brain developmental defect associated with seizure-like electroencephalography spikes, which could be rescued by supplying pyridoxine in embryo water. Both pyridoxine and serine synergistically rescued embryonic developmental defects in zebrafish *got2a* morphants. The two treated individuals reacted favorably to their treatment. Our data provide a mechanistic basis for the biochemical abnormalities in GOT2 deficiency that may also hold for other MAS defects.

Introduction

Infantile-onset encephalopathies with epilepsy often are devastating disorders with major consequences for the life of affected individuals and their families. Identification of an underlying diagnosis is paramount for personalized management. Although inborn errors of metabolism do not represent the most common cause of these encephalopathies, their early identification is of utmost importance, since many require targeted therapeutic measures beyond that of common antiepileptic drugs, either to control seizures or to decrease the chance of neurodegeneration. Here we describe four affected individuals with a metabolic encephalopathy with epilepsy due to a defect in the mitochondrial isoform of glutamate oxaloacetate transaminase or aspartate aminotransferase (GOT; EC 2.6.1.1). This is a pyridoxal 5′-phosphate (PLP)-dependent enzyme that exists as cytosolic (GOT1) and intramitochondrial (GOT2)

[1]Departments of Pediatrics & Clinical Genetics, Emma Children's Hospital, Amsterdam University Medical Centres, Amsterdam Gastro-enterology and Metabolism, University of Amsterdam, 1105 AZ Amsterdam, the Netherlands; [2]Department of Pediatrics / Medical Genetics, BC Children's Hospital Research Institute, Centre for Molecular Medicine and Therapeutics, University of British Columbia, Vancouver, BC V5Z 4H4, Canada; [3]On behalf of "United for Metabolic Diseases," 1105AZ Amsterdam, the Netherlands; [4]Department of Genetics, University Medical Center Utrecht, 3584 EA Utrecht, the Netherlands; [5]Zebrafish Centre for Advanced Drug Discovery, Keenan Research Centre for Biomedical Science, Li Ka Sheng Knowledge Institute, St. Michael's Hospital, Toronto, ON M5B 1T8, Canada; [6]Department of Medicine, Physiology and LMP & Institute of Medical Science, University of Toronto, Toronto, ON M5G 2C4, Canada; [7]Departments of Biochemistry, Molecular Biology and Medical Genetics, Cumming School of Medicine, University of Calgary, Calgary, AB T2N 4N1, Canada; [8]Alberta Children's Hospital Research Institute, University of Calgary, Calgary, AB T2N 4N1, Canada; [9]Department Neurosciences and Pediatric, Howard Hughes Medical Institute, University of California; Rady Children's Institute for Genomic Medicine, San Diego, CA 92093, USA; [10]Department of Molecular Medicine and Al Jawhara Center for Molecular Medicine, Genetics and Inherited Diseases, College of Medicine and Medical Sciences, Arabian Gulf University, Postal Code 328, Bahrain; [11]Clinical Genetics Department, Human Genetics and Genome Research Division, National Research Centre, Cairo 12311, Egypt; [12]Centre for Molecular Medicine and Therapeutics, Department of Medical Genetics, BC Children's Hospital Research Institute, University of British Columbia, Vancouver, BC V5Z 4H4, Canada; [13]Faculty of Pharmaceutical Sciences, University of British Columbia, Vancouver, BC V6T 1Z3, Canada; [14]BC Children's Hospital Research Institute, Vancouver, BC V5Z 4H4, Canada; [15]Laboratory Genetic Metabolic Diseases, Department of Clinical Chemistry, Amsterdam University Medical Centres, University of Amsterdam, Amsterdam Gastro-enterology and Metabolism, 1105 AZ Amsterdam, the Netherlands; [16]CHU Sainte-Justine Research Center, Montreal, QC H3T 1C5, Canada; [17]Department of Neuroscience & Mental Health, The Hospital for Sick Children & Department of Physiology, University of Toronto, Toronto, ON M5G 1X8, Canada; [18]Department of Laboratory Medicine, Translational Metabolic Laboratory, Radboud University Medical Centre, 6525 GA Nijmegen, the Netherlands; [19]Amalia Children's Hospital, Department of Pediatrics, Radboud University Medical Centre, 6525 GA Nijmegen, the Netherlands; [20]Radboud Center for Mitochondrial Medicine, Department of Pediatrics, Radboud University Medical Centre, 6525 GA Nijmegen, the Netherlands
[21]These authors contributed equally to this work
*Correspondence: c.d.vankarnebeek@amsterdamumc.nl (C.D.M.v.K.), ron.wevers@radboudumc.nl (R.A.W.)
https://doi.org/10.1016/j.ajhg.2019.07.015.

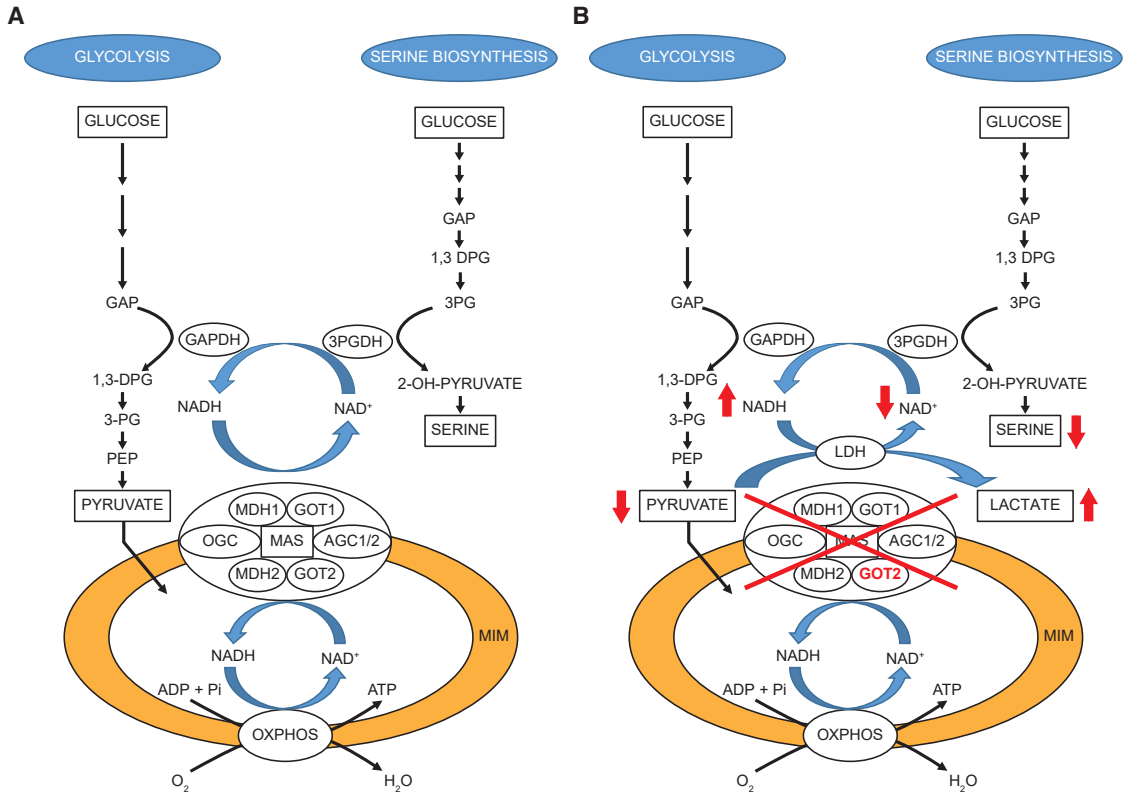

Figure 1. Schematic Diagram Showing the Essential Role of the Malate-Aspartate NAD(H) Redox Shuttle in the Re-oxidation of Cytosolic NADH

(A) The cytosol contains a variety of different NADH-generating dehydrogenases involved in glycolysis, serine biosynthesis, and other pathways. Since the mitochondrion is the ultimate site of NADH-re-oxidation, the NADH generated in the cytosol needs to be shuttled across the mitochondrial membrane. This is brought about by so-called NAD(H) redox shuttles, with the malate aspartate shuttle as the most important one. The malate aspartate shuttle requires the concerted action of six different components: cytosolic and mitochondrial malate dehydrogenase (MDH1 and MDH2), cytosolic and mitochondrial glutamate aspartate transaminase (GOT1 and GOT2), and the two mitochondrial solute carriers aspartate-glutamate (AGC1 and AGC2) and 2-oxoglutarate (OGC).

(B) Schematic diagram showing the consequences of an impairment in the malate-aspartate NAD(H) redox shuttle and the important role of lactate dehydrogenase in the re-oxidation of the NADH generated in the cytosol. GAP, glyceraldehyde 3-phosphate; 1,3-DPG, 1,3-diphosphoglycerate; 3-PG, 3-phosphoglycerate; PEP, phosphoenolpyruvate; GAPDH, glyceraldehyde 3-phosphate dehydrogenase; 3-PGDH, 3-phosphoglycerate dehydrogenase; LDH, lactate dehydrogenase; NAD^+, nicotinamide adenine dinucleotide (oxidized form); NADH, nicotinamide adenine dinucleotide (reduced form); MIM, mitochondrial intermembrane space; ADP, adenosine diphosphate; ATP, adenosine triphosphate; Pi, inorganic phosphate; OXPHOS, oxidative phosphorylation.

isoforms. Both isoforms catalyze the reversible interconversion of oxaloacetate and glutamate into aspartate and α-ketoglutarate. These enzymes are part of the malate-aspartate shuttle (MAS), a key player in intracellular NAD(H) redox homeostasis (Figure 1).[1,2] NADH produced in cytosolic NAD-linked dehydrogenase reactions, mainly during glycolysis, is re-oxidized to NAD^+ inside the mitochondria.[3] Since the inner mitochondrial membrane is relatively impermeable to NAD^+ and NADH,[4] NAD(H)-redox shuttles exist.[3] The MAS provides a mechanism for net transfer of NADH reducing equivalents across the inner mitochondrial membrane.[4] Defects in the MAS have been described due to mutations in genes encoding mitochondrial malate dehydrogenase (*MDH2* [MIM: 154100]) and both aspartate-glutamate carriers (*SLC25A12* [MIM: 603667], *SLC25A13* [MIM: 603859]).[5–9]

We report GOT2 deficiency, a MAS disorder, and present the clinical and biochemical phenotype of three unrelated families, computational analyses, and experimental data to validate the deleterious impact of the identified *GOT2* (MIM: 138150) variants, as well as biomarkers and therapeutic strategies for this inborn error of metabolism.

Material and Methods

The Three Families

Family I was enrolled into the TIDEX gene discovery project (UBC IRB approval H12-00067) and provided written consent for the investigations and for publication of this manuscript. Written informed consent was also obtained for the families II and III.

Whole-Exome Sequencing (WES) Analysis

Family I

Trio (proband-mother-father) whole-exome sequencing (WES) was performed using the Agilent SureSelect kit and Illumina HiSeq 2000 (Perkin-Elmer). The sequencing reads were aligned to the

human reference genome version hg19 using Bowtie 2[10] and mean coverage of 43× (proband), 32× (mother), and 48× (father) was achieved. The data were further analyzed using our semi-automated bioinformatics pipeline:[11] (1) the duplicates were marked and sorted using Picard, (2) variants were called using SAMtools and BCFtools after indel realignment using GATK, (3) transcripts were annotated using snpEff,[12] (4) functional variants were prioritized for rare variants by comparison against the public databases dbSNP, NHLBI Exome Sequencing Project Exome Variant Server, and Exome Aggregation Consortium [ExAC]), and (5) subsequently screened under a series of Mendelian inheritance models: homozygous, hemizygous, compound heterozygous, and *de novo* as described previously.[11] The UCSC Genome Browser was used to examine conservation of the affected amino acids, while the protein domains in which the variants occurred was visualized using the Lollipops software.[13]

Families II and III

WES was performed on affected probands of families II and III. In family II, candidate missense variants were identified in three genes—*MUC19* (MIM: 612170), *GOT2*, and *ZNF157* (MIM: 300024)—consistent with recessive mode of inheritance after filtering and prioritization of the variants. Similarly, missense variants in four genes—*PRKAG3* (MIM: 604976), *GOT2*, *ABCA10* (MIM: 612508), and *DSG3* (MIM: 169615)—were identified in family III. The variant had to be homozygous in all probands with an allele frequency in gnomAD less than 0.01% and in the Greater Middle eastern population of less than 1%. For consanguineous families, the variant was required to be present within the linkage peak as defined by parametric linkage analysis with LOD > 1.4 or in a "run of homozygosity" of at least 1 Mb. In family II, the *GOT2* variant (hg19:16: g.58750636G>C, c.784C>G [p.Arg262Gly], GenBank: NM_002080.2:5166106) was the only variant falling within the linkage peak with LOD > 1.4.

Sequence Alignment

Sequences of GOT2 orthologs were identified using BLAST with the human reference GOT2 protein sequence (GenBank: NP_002071, corresponding to mRNA GenBank: NM_002080); GOT2 orthologs date back as far as yeast. Sequences were selected to cover a large phylogenetic distance. Multiple sequence alignments were calculated using MAFFT global alignment (mafft-ginsi)[14] and visualized using Jalview.[15]

Protein Modeling

The effects of the *GOT2* variants on the protein structure and function were analyzed using three-dimensional protein structures. We modeled the variants based on a template structure of the mature human GOT2 protein, solved as a homodimer complex at 3.0 Å resolution (PDB: 5AX8, chains A and C).[16] As the human structure lacked substrate and cofactor molecules, we also analyzed the mature mouse GOT2 protein (PDB: 3PDB, chains A and B, 2.4 Å)[17] crystallized with oxaloacetate and pyridoxal 5′-phosphate (present in an intermediate state of catalysis as covalently bound to Lys279). The human and mouse sequences and structures are highly similar at 95% sequence identity and an average distance between atoms <1 Å (root-mean-square deviation [RMSD]; superimposition of the protein structures). Therefore, ligand coordinates from the mouse structure were transferred to the human structure. The resulting PDB: 5AX8 template structure with ligands was submitted to SWISS-MODEL to model the GOT2 variants.[18] Models were of overall high quality (global model quality estimation [GMQE] = 0.98). Structures were visualized with YASARA (see Web Resources).

GOT2 Protein Expression

Western blot analysis on mutant and control fibroblasts of GOT2 and succinate dehydrogenase complex flavoprotein subunit A (SDHA, a mitochondrial marker protein) was performed following standard molecular biological procedures. Antibodies used are a GOT2 polyclonal antibody (Bethyl A304-356A-T; diluted 1:1,000) with the secondary antibody Alexa Fluor-680-labeled goat-anti-rabbit antibody (Invitrogen Cat. No. A21109) and a monoclonal complex II SDHA antibody (Abcam cat. ab14715; diluted 1:2,000) with the secondary goat-anti-mouse IRDye800 antibody (Rockland Cat. No. 610-132-121). Western blot analysis on the HEK293 CRISPR/Cas9 cells was performed following standard biological procedures, using the β-actin polyclonal antibody from Sigma (Cat. No. ABT1487; diluted 1:10,000) and the secondary antibody donkey anti-mouse IRD 680.

GOT2 Activity in Skin Fibroblasts

GOT activity was measured in mitochondria-enriched fractions prepared from cultured skin fibroblasts from an affected individual and three control subjects. For this purpose, 1×10^6 cells were cultured in M199 medium supplemented with 10% FBS and antibiotics. Cells were harvested by trypsinization and resuspended in ice-cold 10 mM Tris-Cl (pH 7.6). All subsequent steps were performed at 4°C. The cell suspension was homogenized by using a Potter-Elvehjem homogenizer after which 0.2 vol of 1.5 M sucrose was added. The suspension was centrifuged for 10 min at 600 × *g*. The supernatant was further centrifuged for 20 min at 20,000 × *g*. The mitochondria-enriched pellet was washed twice with 10 mM Tris-Cl (pH 7.6), was resuspended in the same buffer, and was stored at −80°C until measurements were performed. Prior to further measurements, 0.01% Triton X-100 was added and the samples were freeze-thawed for three cycles. Protein concentrations of the extracts were determined on a KoneLab 20XTi system using a U/CSF protein kit (ThermoFisher). GOT activity was measured using a commercial kit (Cat. No. 05531446) from Roche Diagnostics (Roche Diagnostics), for the quantitative determination of glutamate oxaloacetate transferase with pyridoxal 5′-phosphate activation on a Cobas C8000 analyzer (Roche Diagnostics). The assay is based on the following reaction, which is catalyzed by GOT in the mitochondrial protein extracts: 2-oxoglutarate + L-aspartate → L-glutamate + oxaloacetate. This reaction is coupled to the following reaction: oxaloacetate + NADH + H^+ → malate + NAD^+, catalyzed by malate dehydrogenase included in the assay kit. The GOT activity in the sample is directly proportional to the rate of NADH conversion, which is measured spectrophotometrically at 340 nm. The experiment was performed in duplicate.

Generation of GOT2-Knockout HEK293 Clones by CRISPR/Cas9

The CRISPR/Cas9 genome editing technology as described by Ran was used to introduce a disruption of the *GOT2* gene in HEK293 cells.[19] Oligonucleotide sequences coding for a guide RNA upstream of a proto-spacer adjacent motif (PAM) site in exon 2 (5′-CCT, c.197_199) of *GOT2* are available upon request. The two oligos were annealed and subsequently cloned into the pX458 (-pSpCasq(BB)-2A-GFP) plasmid,[19] followed by Sanger

sequencing of the insert to confirm the correct sequence. HEK293 cells were transfected with 2 μg plasmid, and single green fluorescent protein (GFP)-positive cells were sorted into wells of a 96-well plate using fluorescence-activated cell sorting (FACS) flow cytometry (S800H Cell Sorter, Sony) as described.[19] After 3–4 weeks, DNA was isolated from the expanded single colonies, and exon 2 of the *GOT2* gene was PCR amplified using Phire Hot Start II DNA Polymerase (ThermoFisher Scientific) according to the manufacturer's instructions and subsequently Sanger sequenced. Three clonal CRISPR/Cas9 GOT2-knockout HEK293 cell lines were generated: clone A3 was compound heterozygous for 205dup/202_203insA, clone A6 for 205del/190_206del/203_206dup, and clone A7 homozygous for 205dup. There were no significant putative off-target regions predicted by the online CRISPR design tool.

GOT2 Activity in the HEK293 CRISPR/Cas9 Cells

The GOT activity, in the HEK293 cells, was measured spectrophotometrically using a coupled assay method based on the NADH-dependent conversion of oxaloacetate as generated from L-aspartate by GOT, to malate mediated by malate dehydrogenase added to the assay mixture. The absorbance at 340 nm was followed for 30 min at 37°C using a centrifugal analyzer (Hoffman COBAS-FARA, Hoffman, LaRoche). The composition of the assay mixture was as follows: 100 mM potassium phosphate buffer (pH 7.4); 100 mM L-aspartate; 0.2 mM NADH; 0.1% (w/v) Trition-X-100; 7.3 U/mL malate dehydrogenase and 25 μL of cellular homogenate, in a final volume of 250 μL. The reactions were started by adding 10 mM α-ketoglutarate to the assay mixture.

Lentiviral Transduction of Mutant Fibroblasts with Wild-Type GOT2

A synthetic GOT2 cDNA (GenBank: NM_002080) with stop codon and attB sites was obtained from Thermo Fisher (ThermoFisher Scientific). The DNA fragment was cloned into pDONR201 and subsequently into pLenti6.2/V5-DEST by Gateway technology cloning (Invitrogen). The resulting expression construct was checked by Sanger sequencing. The construct was used for lentiviral particle production by transfection into HEK293-FT cells, as described before.[20] The viral particle-containing supernatant was used to transduce subconfluent fibroblasts with *GOT2* mutations. After selection with blasticidin (Invivogen), the resulting cell culture was used for western blot and GOT enzyme activity assays. As a control, the mutant cells were transduced with lentiviral particles from HEK293 cells transfected with a pLENTI construct with a green fluorescent protein cDNA, as described before.[20]

Cell Culture

Dulbecco's modified eagle medium (DMEM), high glucose, GlutaMAX, pyruvate (Cat. No. 31966); DMEM-no glucose (Cat. No. 11966); fetal bovine serum (FBS; Cat. No. 10270); penicillin-streptomycin (P/S (10,000 U/mL); Cat. No. 15140) and trypsin-ethylenediaminetetraacetic acid (trypsin-EDTA (0.5%), no phenol red; Cat. No. 15400) were purchased from GIBCO (ThermoFisher Scientific). Uniformly labeled $^{13}C_6$-glucose (99%) was purchased from Cambridge Isotope Laboratories. Glucose was purchased from Sigma-Aldrich.

Fibroblasts and HEK293 cells (GOT2-WT; and GOT2-A3, -A6, and -A7 knockout clones) were grown in 75 cm^2 flasks and maintained in DMEM, high glucose, GlutaMAX, pyruvate (with 10% heat-inactivated FBS and 1% P/S), in a humidified atmosphere of 5% CO_2 at 37°C. Cells were passaged upon reaching confluence and media was refreshed every 48 h.

Stable Isotope Analysis: *De Novo* Serine Biosynthesis

Cells were plated on 6-well plates (500,000 cells per well) and allowed to grow for 4 days. Media was refreshed 24 and 72 h after plating. On the fourth day, cells were either incubated with DMEM medium without glucose (DMEM, Cat. No.11966; supplemented with 10% FBS and 1% P/S), to which 25 mmol/L glucose or 25 mmol/L uniformly labeled $^{13}C_6$-glucose was added. Cells were harvested at $t = 0$, 0.5, 4, and 10 h. To this end, cells were washed twice with cold PBS (4°C) and harvested by scraping with 1.5 mL ice-cold methanol. The samples were transferred into a 1.5 mL eppendorf tubes, centrifuged (16,200 × *g* for 10 min at 4°C) and the supernatants were transferred to new 1.5 mL eppendorf tubes. The samples were evaporated at 40°C under a gentle stream of nitrogen until complete dryness and reconstituted with 500 μL of UPLC-grade methanol (room temperature). The reconstituted samples were stored at −80°C until amino acid analysis was performed.

Recovery Studies on *De Novo* Serine Biosynthesis

The recovery studies on serine *de novo* biosynthesis were performed by incubating cells with DMEM-no glucose medium, to which we added 25 mmol/L $^{13}C_6$-glucose, and 0, 2.5 or 5 mmol/L of glycerol or pyruvate. Samples were collected as described before, at $t = 0$, 0.5, and 4 h.

Amino Acid Analysis

To quantify intracellular $^{13}C_3$-serine and $^{13}C_2$-glycine, we adapted the UPLC-MS/MS method described by Prinsen et al.[21] Apart from not using internal standards to avoid interference with the signal of $^{13}C_3$-serine and $^{13}C_2$-glycine, adapting the range of the calibrators to our samples' concentrations, and using quality control (QC) samples that resembled the concentrations of our samples, no further adaptations were needed for sample preparation or analysis of the amino acids.

Generation of GOT$^{-/-}$ Mice by CRISPR/Cas9

The following mutations GenBank: NM_002080.2:c.617_619delTCT (p.Leu209del) and c.1009C>G (p.Arg337Gly) were introduced into the mouse genome using the CRISPR/Cas9 method (Table S3). The gRNAs were selected using the Crispr guide selection software from Feng Zhang's laboratory (Web Resources; Table S4). The gRNAs were subcloned into the pX330-U6-Chimeric_BB-CBh-hSpCas9, a gift from Feng Zhang (Addgene plasmid #42230). Repair templates (ssODN) were designed to insert the desired mutations and ultramer DNA were synthesized by Integrated DNA Technologies (IDT). The Got2emhD335fs14* was generated while making Got2emhR337G mice as a results of unrepair indels. Both mice were generated by the Institut de Recherches Cliniques de Montréal (IRCM). Briefly, about 2 picoliter of ssODN (100 μL/ng) and pX330-U6-Got2-hSpCas9 plasmid (10 ng/μL) in 5 mM Tris, 0.02 mM EDTA was microinjected into a pronucleus of C57BL/6J or B6C3F1 mouse zygotes that were transferred into the oviduct of CD-1 pseudopregnant surrogate mothers according to the standard approved animal user protocols IRCM 2014-17. The Got2emhL209del was generated by the McGill transgenic core facility. Briefly, the gRNA was transcribed *in vitro* using the MAXIscript T7 kit (ThermoFisher, AM1312). About 2 picoliter of gRNA (20 ng/μL), ssODN (100 ng/μL), and

Cas9 RNA (50 ng/μL) were microinjected into a pronucleus of C57BL/6N mouse zygotes and subsequently implanted in CD-1 pseudopregnant surrogate mothers according to the standard approved animal user protocols #4437.

After weaning, the mice were transferred to the Centre de Recherche du Centre Hospitalier Universitaire (CR-CHU) of Sainte-Justine Hospital. Mouse husbandry and experiments were done according to the approved animal user protocols #541 by the Coordonnatrice du Comité Institutionnel des Bonnes Pratiques Animales en Recherche (CIBPAR). This committee is following the guidelines of the Conseil Canadien de la Protection des Animaux (CCPA).

Zebrafish Husbandry

Zebrafish were maintained at 28.5°C in a 10/14-h dark/light cycle. Protocols for experimental procedures were approved by the Ethics Board at St. Michael's Hospital, Toronto, Canada (Protocol ACC660).

Morpholino Knockdown

To knock down gene expression, we designed and injected oligonucleotide morpholinos targeting the first ATG start codon as well as the splicing (sp) donor site of the exon 2 for *got2a*. A standard control MO (Cont MO) was used as control. The MO sequences are as follows: *got2a* atg-MO, 5′-CTTGCTGGATTTGAACAGGGCCATT-3′; *got2a* sp-MO, 5′-AGCTATTTAATATCACACCTTTCGA-3′; and standard control MO, 5′-CCTCTTACCTCAGTTACAATTTATA-3′.

MOs were designed by Gene Tools. Normally we injected individually 4 nL of *got2a atg* (8 ng/μL) and 4 nL of *got2a sp* (16 ng/μL) MOs. Each injection was repeated at least three times. For phenotype severity rescue experiments, ATG-blocking MO solutions were prepared at 0.4 mM final concentration. 2 nL of MO solution was injected in each embryo. For survival rescue experiments, 4 nL of 0.8 mM MO solution was used.

Molecular Validation of got2a Splicing Morpholino Knockdown

Knockdown of *got2a* with sp-MO was confirmed by RT-PCR. Embryos were injected at 1 cell stage with 4 nL of *got2a* sp-MO (16 ng/μL), the MO was diluted in water and phenol red. At 24 hpf, embryos were manually dechorionated. Total RNA was extracted from embryos at 24 and 48 hpf using TRIzol (Invitrogen). The RNA concentration of each sample was quantified using a NanoDrop ND-1000 spectrophotometer (NanoDrop Technologies). RNA integrity was verified in 1% agarose gel electrophoresis (Invitrogen). The RNA template was converted into cDNA using Superscript II reverse transcriptase (Invitrogen). The primers used are as follows: forward primer, 5′-GCAATGGCCCTGTTCAAATC-3′; reverse primer, 3′-CTGCATGCCTGCATCTCTAA-5′.

Compound Rescue Experiments

Pyridoxine (P5669), serine (S4375), sodium pyruvate (P2256), and L-proline (P0380) were purchased from Sigma-Aldrich. Zebrafish embryos were distributed in 24-well plates (10 embryos per well per condition). At 6 hpf, the embryos were treated with one of the following compounds: 25 mM of pyridoxine, 2 mM of serine, 0.5 mM of sodium pyruvate, and 0.2 mM of L-proline. The plates were kept at 28°C. Survival and phenotypic assays were performed at 1, 2, and 3 day post fertilization (dpf). The compound solutions were replaced with the corresponding fresh solutions at 1 and 2 dpf. For survival assay, heartbeat and embryo movement were considered at 2 dpf. For phenotypic assay, five phenotypes (P1, P2, P3, P4, and P5) were characterized at 3 dpf based on the severity (Figure 5A). For phenotype severity calculation, the following "phenotype scores" were used: P0 (normal) = 0, P1 = 1, P2 = 2, P3 = 3, P4 = 4, P5 (dead) = 5. Average phenotype severity was calculated with the following formula:

$$\text{Average phenotype severity} = \sum \text{n x (Phenotype score)/N}$$

where n = number of embryos showing a specific phenotype in a well, N = total initial number of embryos in a well. Treated samples were compared to non-treated conditions using one-way ANOVA test.

Electroencephalogram (EEG)

EEG recordings of zebrafish embryos were performed according to a previously reported method.[22,23] Low melting 1.2% agarose (BioShop) was placed within recording media solution (1 mM NaCl, 2.9 mM KCl, 10 mM HEPES, 1.2 mM $MgCl_2$, 10 mM dextrose, 2.1 mM $CaCl_2$). Embryos were anesthetized with 0.02% tricaine (Sigma Aldrich). Embryos in the agarose block were immersed in recording media solution. A microelectrode (1 μm diameter, 2–7 MΩ) was mounted on a micromanipulator and inserted into the front brain of zebrafish embryo at 2 dpf. Microelectrodes were fabricated from 1.5 mm OD borosilicate glass and pulled into two needles with a two-step Narishige micropipette puller. The microelectrode was back loaded with recording media solution using a 1 mL syringe with a Corning syringe filter (0.2 μm), and a 28-gauge MicroFil filament (World Precision Instruments) was attached. Electrical activity was captured with an Axopatch 200B (Axon Instrument) patch clamp amplifier in current clamp mode. Data were collected in pClamp 8 software (Molecular Devices) in gap-free acquisition mode, sampling at 10 kHz, and gain at 100 mV/pA. A recording chamber and electrophysiology rig were used to stabilize embryos. EEG was analyzed as number of events and duration of each event for a single embryo. The average of number of evens and event duration were calculated for each embryo.

Rescue of Seizures in got2a sp-MO by Pyridoxine

At 2 h after *got2a* sp-MO injection, 25 mM of pyridoxine was added to the embryo water in a 12-well plate and incubated at 28°C. After 24 h of incubation, chorions were removed manually. The medium and pyridoxine were refreshed after 24 hpf. At 48 hpf, the embryos were analyzed by electroencephalogram.

Results

Clinical History

Four individuals from three unrelated families (P1–P4; Table 1; families I, II, and III; Figures 2A–2C) suffered from similar clinical features, albeit of different severity: progressive microcephaly, failure to thrive and feeding difficulties, a metabolic encephalopathy with epilepsy from the first year of life, and subsequent intellectual and motor disabilities. Cerebral imaging showed cerebral atrophy and white matter abnormalities in all four individuals. Biochemically, high plasma lactate and hyperammonemia were found. In individual 1, who was most severely affected, plasma serine was low and citrulline high; his seizure control

Table 1. Clinical, Biochemical, and Genetic Characteristics of the GOT2-Deficient Individuals

	Individual 1, Family 1	Individual 2, Family II	Individual 3, Family II	Individual 4, Family III
Clinical History				
Gender	M	F	F	M
Age (years)	8	10	8	4
Ethnicity	Romanian	Egyptian	Egyptian	Egyptian
Parental consanguinity	–	+	+	+
Unaffected siblings	0	1	1	0
Siblings	first child was stillborn	first child spontaneous abortion	first child spontaneous abortion	sister died at age of 5 months
Delivery	Caesarean section	NVD	NVD	NVD
Gestational age (weeks)	38	32	38	39
Birth length percentile	85th	<1st	5th	50th
Birth weight percentile	3rd	<1st	5th	5th
Birth HC percentile	5th	<1st	15th	15th
Apgar scores	9	5	8	6
Neonatal period	–	artificial ventilation (first 20 days)	–	–
Hypotonia (neonatal)	+	+	+	+
Neonatal feeding difficulties	+	+	+ (mild)	+
Frequent infections	+	+	+	+
Seizure onset	9 months	7 months	6 months	4 months
Seizure frequency	10–100 per day	daily	daily	20 per day
Seizure semiology	upward gaze, clonic seizures at upper limbs (left ± right), head tilting to left, and facial clonic movements	myoclonic, GTC, tonic	myoclonic, GTC	myoclonic, tonic with upward gaze
Pyridoxine supplementation	+	–	–	+
Serine supplementation	+	–	–	+
Progressive microcephaly	+	+	+	+
MRI findings	multicystic encephalomalacia, cerebral atrophy	mild cerebral atrophy with a hypoplastic vermis and a thin corpus callosum	mild cerebral atrophy with a hypoplastic vermis and a thin corpus callosum	(mainly frontoparietal) asymmetric dilated lateral ventricles; hypoplastic vermis; corpus callosum hypoplasia
EEG findings	–	tempoparietal spikes	tempoparietal spikes	bilateral frontoparietal frequent spikes
Metabolic Screening				
Age	14 months	10 years	8 years	4 years
Amino acids (blood)	abnormal	normal	normal	normal
Serine (ref. value) (μmol/L)	47 (70–294)	114 (88–172)	171 (88–178)	130 (88–178)
Glycine (ref. value) (μmol/L)	280 (80–340)	184 (167–338)	295 (156–328)	273 (156–328)
Citrulline (ref. value) (μmol/L)	89 (7–55)	37 (20–46)	36 (21–43)	27 (21–43)
Organic acids (urine)	normal profile	normal profile	normal profile	normal profile
Acylcarnitine (blood)	normal profile	normal profile	normal profile	normal profile

(*Continued on next page*)

Table 1. ***Continued***

	Individual 1, Family 1		Individual 2, Family II	Individual 3, Family II	Individual 4, Family III
Clinical Chemistry					
Age	8 months		9 years	7 years	3 years
Blood lactate (ref. value) (mmol/L)	5.7 (0.7–2.1)		4.2; 3 (0.5–2.2)	3.9 (0.5–2.2)	4.5 (0.5–2.2)
Blood ammonia (ref. value) (μmol/L)	143 (16–60)		110 (<80); 70 (11–32)	120 (<80)	120 (<80)
Last visit					
Age	7 years		10 years	8 years	4 years
Length percentile	$<1^{st}$		$<1^{st}$	$<1^{st}$	25^{th}
Weight percentile	$<1^{st}$		$<1^{st}$	1^{st}	25^{th}
HC percentile	$<3^{rd}$		$<1^{st}$	$<1^{st}$	$<1^{st}$
Intellectual disability	profound		severe	severe	profound
Speech	no words		<10 single words	no words	no words
Motor disability	severe spastic quadriplegia, wheelchair bound		spastic paraparesis, walks short distances with support	spastic paraparesis, wheelchair bound	severe spastic quadriplegia, wheelchair bound
GOT2 variants					
	compound heterozygous		homozygous	homozygous	homozygous
amino acid change	p.Leu209del	p.Arg337Gly	p.Arg262Gly	p.Arg262Gly	p.Gly366Val
***In silico* Prediction**					
CADD	23.0	23.8	32.0	32.0	33.0
PROVEAN; cutoff: −2.5	na	−4.25 (“damaging”)	−6.7 (“damaging”)	−6.7 (“damaging”)	−8.54 (“damaging”)
PolyPhen2	na	0.922 (“possibly damaging”)	1.0 (“probably damaging”)	1.0 (“probably damaging”)	0.993 (“possibly damaging”)
SIFT; cutoff: 0.05	na	0.243 (“tolerated”)	0 (“damaging”)	0 (“damaging”)	0 (“damaging”)

M, male; F, female; C-section, Caesarean section; NVD, normal vaginal delivery; NICU, neonatal intensive care unit; GTC, generalized tonic-clonic seizures; EEG, electroencephalogram; MRI, magnetic resonance imaging; HC, head circumference; na, not available.

and neurodevelopment improved considerably on pyridoxine and L-serine supplementation to the extent that antiepileptic drugs could be stopped (Supplemental Note, Table 1). Also, individual 4 in whom treatment was started reacted favorably. His seizures diminished on pyridoxine only and were fully controlled by the combined treatment with pyridoxine and serine supplementation (Supplemental Note).

Exome Sequencing and Protein Structural Modeling to Identify GOT2 Damaging Mutations

Nine candidate genes with rare, non-synonymous genetic variants were identified by Trio WES on family I. *GOT2* was considered the best candidate to explain the biochemical phenotype of the proband. The gene contained (1) a paternally inherited in-frame deletion hg19:16: g.58752177 delGAA (p.Leu209del [c.617_619delTTC], GenBank: NM_002080) and (2) a maternally inherited missense mutation hg19:16 g.58749928G>C (p.Arg337Gly [c.1009C>G]). Both variants are not present in dbSNP (version 142), NHLBI ESP, ExAC, gnomAD, or in our in-house genome database comprising more than 11,450 exome and genome sequences. Exome sequencing was also used for the probands of the other families. Three homozygous candidate missense variants were prioritized in the probands in family II and four in family III. Homozygous *GOT2* missense variants for the families II and III were hg19:chr16: g.58750636G>C (c.784C>G [p.Arg262Gly], GenBank: NM_002080) and g.58743394C>A (c.1097G>T [p.Gly366Val]), respectively. The allele frequencies in gnomAD were <0.01% and, within gnomAD, in the Greater Middle Eastern population <1%. The presence and family segregation of all *GOT2* variants was confirmed with Sanger sequencing.

All variants affect evolutionary highly conserved amino acids (Figures 2D, S1, and S2, and Supplemental Data). They are predicted to be damaging by *in silico* methods (Table 1).[24–27] Modeling of the variants in the GOT2 3-dimensional protein structure (Figure 2E) suggests that they reduce the catalytic activity of the enzyme and may impact the overall protein conformation, both of which may result in reduced levels of functional protein (Figure 2E; detailed analysis in Supplemental Data).

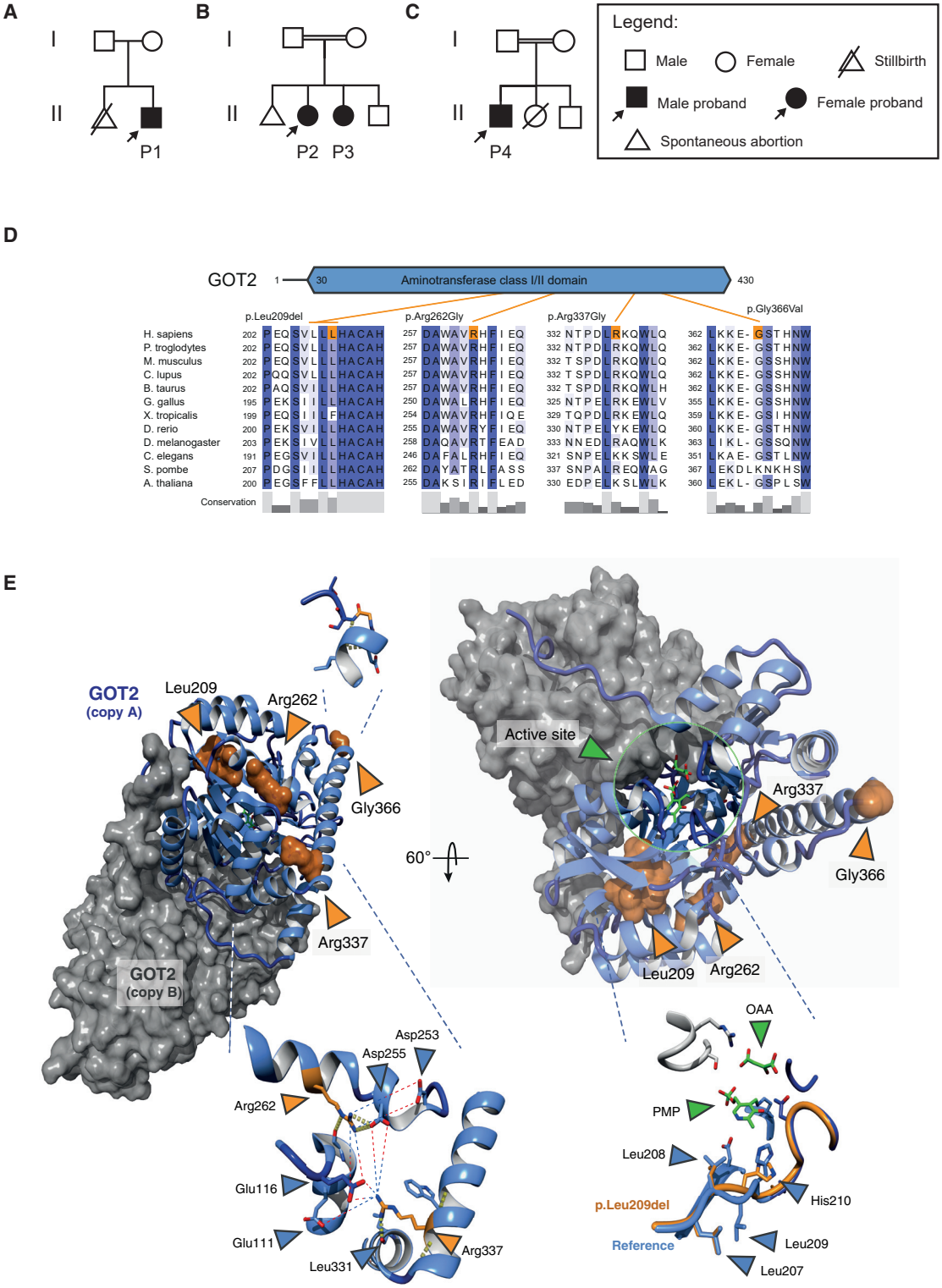

Figure 2. The Pedigrees and the GOT2 Variants

(A–C) Pedigrees of the families I–III.

(D) Alignment of GOT2 ortholog sequences. p.Leu209del represents the deletion of a leucine in a tri-leucine stretch. Figure S1 shows the full alignment.

(E) Molecular modeling of the variants. Shown are rotated overview structures of the GOT2 homodimer complex, with variants found in affected individuals shown in orange. Insets: p.Gly366Val (top left), p.Arg337Gly and p.Arg262Gly (bottom left; glycine substitutions not visible), p.Leu209del (bottom right; reference structure in blue and variant model in orange superimposed). While visualized in a single structure, variants are not simultaneously present in the same copy of the gene. Models are based on template structure PDB: 5AX8, with ligand coordinates taken from PDB: 3PDB. PMP, pyridoxamine 5′-phosphate; OAA, oxaloacetate. Hydrogen bonds in yellow; other charge interactions as dashed lines. p.Leu209del shortens a beta strand in the protein core close to the active site, leading to a

(legend continued on next page)

GOT2 Deficiency in Fibroblasts and GOT2-Knockout HEK293 Cells

Western blot analysis revealed that GOT2 was strongly deficient in fibroblasts of individual 1 and to a lesser extent in individuals 2–4 (Figure 3A). Three clonal CRISPR/Cas9 GOT2-knockout HEK293 cell lines were successfully generated: clone A3 was compound heterozygous for 205dup/202_203insA, clone A6 for 205del/190_206del/203_206dup, and clone A7 was homozygous for 205dup. Western blot analysis performed on the three clonal cell lines showed that GOT2 was not detectable in any of the clones (Figure 3B).

GOT2 enzymatic activity was determined in mitochondria-enriched fractions. In individuals 1–4 it amounted to 8%, 21%, 21%, and 18% of the mean of control subjects, respectively. The two GOT2-carriers (1 and 2) had a residual activity of 39% and 62%, respectively (Figure 3C). GOT enzymatic activity measurements in whole-cell lysates prepared from the three different GOT2-knockout clonal cell lines, which includes the combined activity of both GOT1 and GOT2, was found to be markedly decreased ($p < 0.01$) compared to GOT activity in wild-type cells (Figure 3D). In addition, GOT2 activity in the mitochondrial fraction was less than 2% of the activity measured in control mitochondrial fractions (Figure 3E).

To investigate whether the defect could be rescued by wild-type GOT2 cDNA, fibroblasts of individual 1 were transduced using lentiviral particles with wild-type GOT2. After selection of transduced cells, GOT enzyme activity was measured in mitochondrial preparations showing a strong increase of the mitochondrial GOT activity to levels that fall within the range measured in control cells. The control transduction experiment showed little or no effect on GOT2 activity of the cells (Figure 3F).

De Novo Serine Biosynthesis in Fibroblasts and GOT2-Knockout HEK293 Cells

Because the most important clinical finding in individual 1 were serine- and pyridoxine-responsive seizures, we evaluated the impact of GOT2 deficiency on *de novo* serine biosynthesis. Formation of stable isotope-labeled serine from labeled glucose was analyzed in fibroblasts of all GOT2-deficient individuals, two GOT2 carriers, six control subjects, and fibroblasts from individuals with a defect in serine biosynthesis (phosphoserine aminotransferase deficiency [PSATD] [MIM: 610992] and 3-phosphoglycerate dehydrogenase deficiency [3-PDGHD] [MIM: 608015]). The fibroblasts of the GOT2-deficient individuals 1 and 4 formed less $^{13}C_3$-serine amounting to 34% and 33% of control subjects, respectively. Individuals 2 and 3 produced 55% and 52% of control subjects, respectively. In addition, the GOT2-carrier 1 produced 66% of $^{13}C_3$-serine, while the GOT2-carrier 2 produced almost as much as control s (81%). In fibroblasts from 3-PGDHD- and PSATD-deficient individuals, *de novo* serine biosynthesis amounted to 15% and 0%, respectively (Figure 4A).

Analysis of *de novo* serine biosynthesis in GOT2-knockout cell lines revealed that the three GOT2-knockouts had a severe reduction in $^{13}C_3$-serine production (90%–93%). In addition, $^{13}C_2$-glycine synthesis was reduced by 87%–88% (Figure 4B).

We hypothesized that the GOT2 defect would result in decreased MAS activity resulting in an increased NADH/NAD^+ ratio in the cytosol. To investigate whether restoring the cytosolic redox imbalance would correct the serine biosynthesis capacity of the cells, we incubated the GOT2-knockout cell line A3 with glycerol and pyruvate. Supplementation of the culture medium with 2.5 and 5 mmol/L glycerol had no effect on serine biosynthesis. However, serine and glycine synthesis was fully restored when cells were incubated with 2.5 or 5 mmol/L pyruvate, the substrate of lactate dehydrogenase (LDH; Figures 4C and 4D). This effect is explained by the re-oxidation of cytosolic NADH by LDH.

CRISPR/Cas9 Got2-Knockout Mice

We generated mice heterozygous for the p.Arg337Gly and p.Leu209del mutations, and for a loss-of-function mutation (p.Asp335fs14*). These mice were viable and healthy, similarly to the parents of the four affected individuals. Unfortunately, no homozygous mice for any of these mutations were viable beyond early pregnancy (Table S5). Mouse embryonic fibroblasts (MEFs) were collected at the age of 14 days post coitum (dpc) and genotyped. No homozygous embryos were found suggesting early lethality for all three mutations in mice (Table S6).

Knockdown of got2a in Zebrafish Affects Embryonic Development and Provokes Seizure-like EEG Spikes, which Is Rescued by Pyridoxine and Serine

While CRISPR-based gene knockout is currently widely used to study gene function, however, gene knockdown technologies are still vital methods evaluating gene contribution to diseased phenotypes as the majority of human gene mutations retain residual gene activities at various degrees. Furthermore, there are essential genes that could not be fully knocked out in the organism and *GOT2* could be one of these genes. Using the morpholino-based gene knockdown strategy, our previous studies had led to functional characterization of a number of genes in metabolic diseases.[28,29] As the knockout of *Got2* in mice is embryonic lethal, we knocked down the zebrafish mitochondrial *got2a* gene by ATG- and splicing-blocking morpholinos (MO) (see Figure S3 for details regarding specificity of

repositioning of loops involved in the geometry of the catalytic pocket, likely affecting binding of both the enzyme cofactor (pyridoxal 5′-phosphate) and substrates. p.Gly366Val has a predicted marginal effect on the protein structure, but is still well conserved across evolution. For p.Arg337Gly and p.Arg262Gly, substitution of the positively charged arginine residues with the neutral glycine residue results in a disruption of electrostatic interactions that in the wild-type protein stabilize the α-helical organization of the protein.

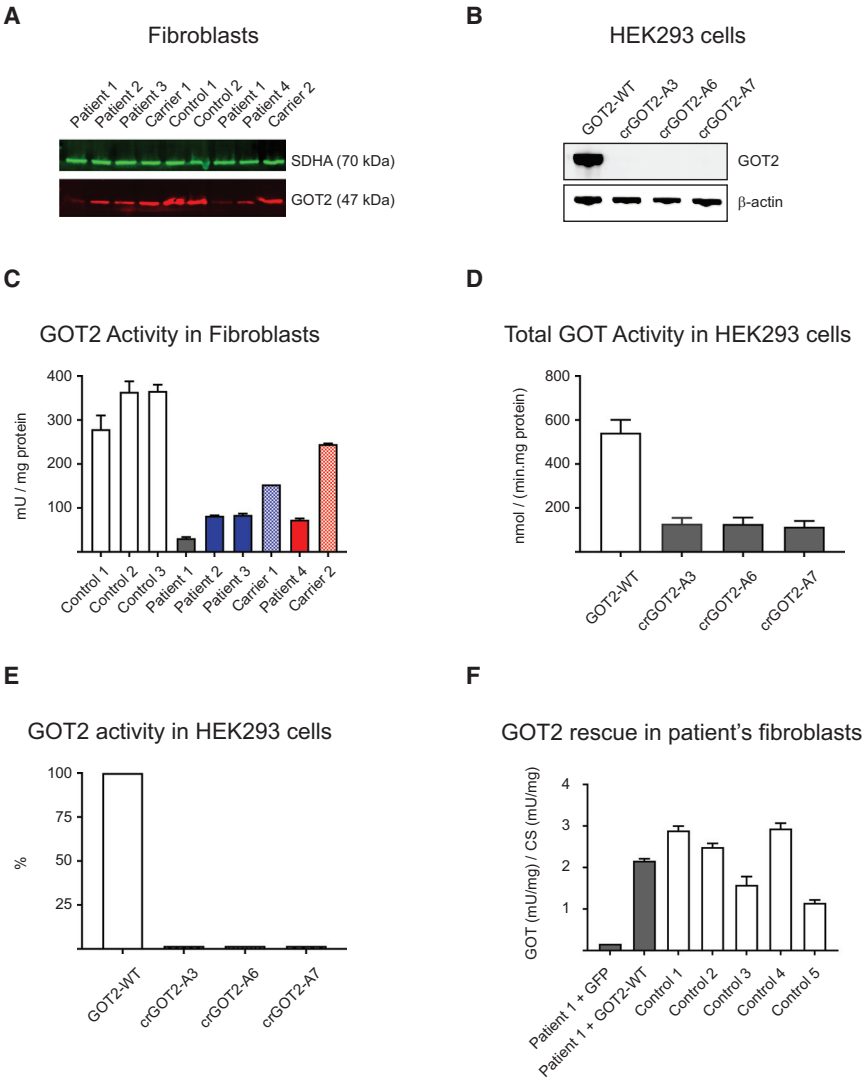

Figure 3. GOT Expression and Activity
(A) Western blot showing GOT2 and the mitochondrial fraction marker SDHA (succinate dehydrogenase complex flavoprotein subunit A) in the GOT2-deficient individuals, GOT2 carriers, and two control fibroblast lines.
(B) Western blot for GOT2 protein in GOT2 wild-type and the three GOT2-knockout HEK293 cell lines.
(C) GOT2 activity in mitochondria-enriched fractions from fibroblasts from the GOT2-deficient individuals, GOT2 carriers, and three healthy control subjects. Graph bars represent mean ± SD.
(D) Total GOT (GOT1 and GOT2 isoforms) activity in whole-cell lysates; results are representative of two independent experiments.
(E) GOT2 activity in the mitochondria-enriched fractions of GOT2-WT and the three GOT2-knockout HEK293 cell lines; results are representative of two independent experiments.
(F) GOT2 rescue experiment in fibroblasts from individual 1. GOT2 activity is restored to control levels when GOT2-deficient fibroblasts are transduced with the *GOT2* wild-type gene. Five control fibroblast lines and the GOT2-deficient fibroblasts transduced without *GOT2* wild-type (+ GFP lane) were used for comparison.

knocking down *got2a*). While 18% of the embryos injected with *got2a* MO showed a mild phenotype at 48 h post fertilization (hpf), many other morphants showed a small head, slow circulation, bend body, and pericardial edema. Bright field imaging confirmed brain developmental defects (Figure 5A). To establish a quantitative measure for rescue of the *got2a*-MO phenotypes, we developed a scoring system to define the phenotype severity in five categories from P1 to P5 (very mild to embryonic death, Figure 5A). In exploring therapeutic methods, we dosed various concentrations and combinations of pyridoxine (PN), serine, pyruvate, and proline in embryo water of the *got2a* morphants. In non-toxic doses to embryos, 25 mM PN and 2 mM serine significantly rescued the phenotype severity ($p < 0.01$). PN and serine had a synergistic effect (3 mM PN + 0.25 mM serine); noticeably 0.5 mM pyruvate also has some rescuing effect ($p < 0.05$; Figure 5B). However, only PN and serine rescue the survival phenotype as scored by beating hearts (Figure 5C).

As epilepsy and seizures are a predominant feature in the four affected individuals, we performed EEG measurements on zebrafish *got2a* morphants. This showed seizure-like spikes when the electrical probe was placed in the forebrain (Figure 5D) but not when placed in the midbrain (data not shown). Interestingly, the frequency of the seizure-like spike discharge events in *got2a* morphants was rescued by supplying PN in the water of the developing embryos as demonstrated by 5 min EEG recording (Figure 5E, left), whereas duration of the events was rescued partially by PN (Figure 5E, right), further supporting the therapeutic strategies in affected individuals.

Discussion

GOT2 deficiency is a mitochondriopathy and our studies demonstrate that it is amenable to therapeutic intervention. Further experience on more affected persons is needed to confirm this. Clinically it presents as an early-onset metabolic encephalopathy with epilepsy, progressive microcephaly, and several biochemical abnormalities. GOT2 deficiency adds to the short list of mitochondriopathies responding to a specific pharmacological intervention.[30] If confirmed on other persons, GOT2 deficiency will expand the list of treatable metabolic epilepsies, recently reported 73 in number,[31] as well as the growing

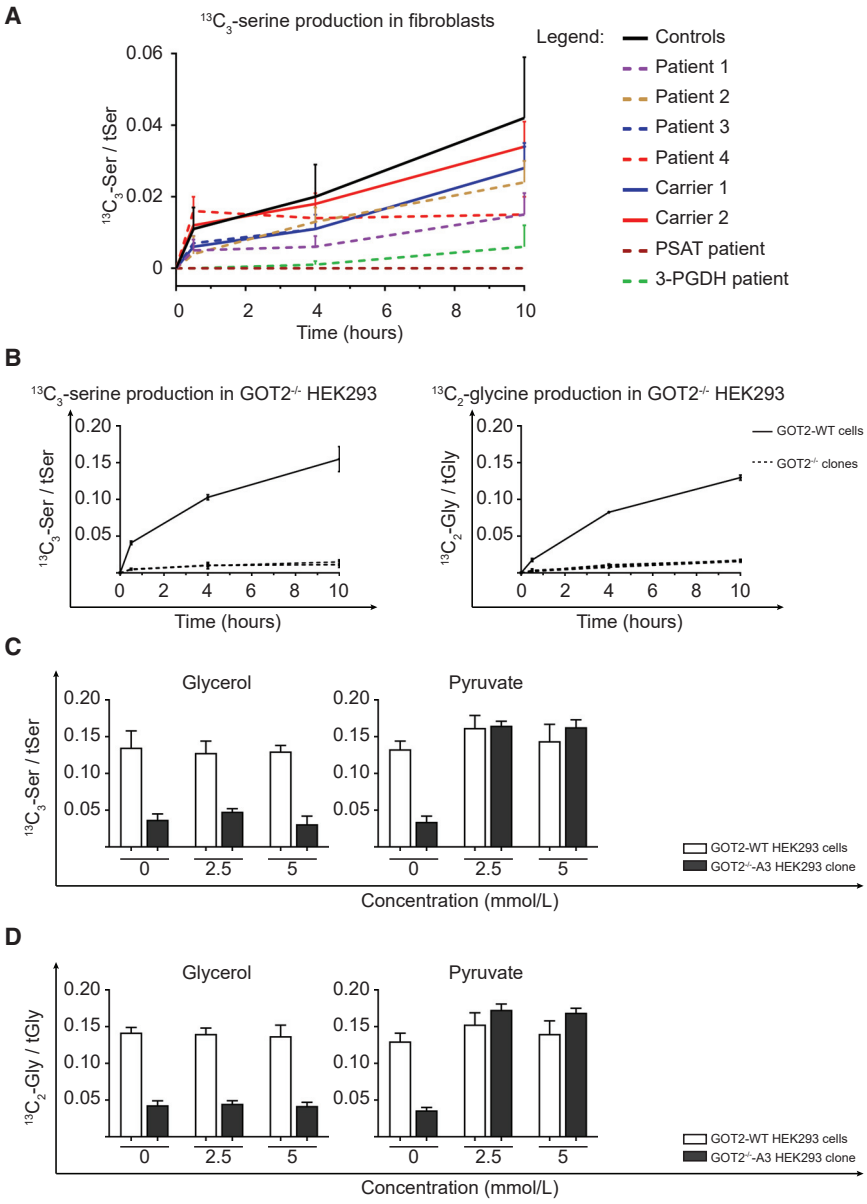

Figure 4. *De novo* Serine Biosynthesis in Mutant Fibroblasts and GOT2-Knockout HEK293 Cells

(A) $^{13}C_3$-serine fractions were determined in fibroblasts of GOT2-deficient cases, the two GOT2 carriers, six healthy control subjects, and two individuals with a *de novo* serine biosynthesis defect (3-PGDHD and PSATD deficiencies). Fibroblasts were incubated with $^{13}C_6$-glucose, and the formation of the labeled $^{13}C_3$-serine was analyzed at t = 0, 0.5, 4, and 10 h after exposure. The results are normalized to total protein content and represented as the mean of n = 3 ± SD for individual 4 and carrier 2, PSATD deficiency and 3-PGDHD deficiency; n = 6 ± SD for individuals 1, 2, and 3, and carrier 1; and n = 33 ± SD for control subjects.

(B) $^{13}C_3$-serine and $^{13}C_2$-glycine fractions were determined in GOT2-WT (full line) and the GOT2-knockout HEK293 cell lines (dashed line). Cells were incubated with $^{13}C_6$-glucose, and the formation of the labeled $^{13}C_3$-serine and $^{13}C_2$-glycine was analyzed at t = 0, 0.5, 4, and 10 h after exposure. The results are representative of two independent experiments and are normalized to total protein content and represented as the mean of n = 3 (biological triplicates) ± SD.

(C) To study the impact of glycerol and pyruvate supplementation in *de novo* serine production of the GOT2-knockout cell lines, we supplemented the cells with these compounds (2.5 and 5 mmol/L) for 4 h. The formation of labeled $^{13}C_3$-serine was analyzed at t = 0, 0.5, and 4 h after exposure. The results are normalized to total protein content and represented as the mean of n = 3 ± SD.

(D) The same study was performed for glycine. The formation of labeled $^{13}C_2$-glycine was analyzed at t = 0, 0.5, and 4 h after exposure. The results are normalized to total protein content and represented as the mean of n = 3 ± SD.

group of pyridoxine and/or pyridoxal 5′-phosphate responsive epilepsies (*ALDH7A1*, *PNPO*, *PLPBP*, *ALPL* [MIM: 107323, 603287, 604436, 171760]).[32] The importance of a thorough metabolic workup including a diagnostic and therapeutic trial with pyridoxine and the active cofactor pyridoxal 5′-phosphate cannot be overemphasized. In each of the three families a child died either during pregnancy, at birth, or at very young age. All affected individuals in this study have some residual GOT2 enzymatic activity, which is probably essential for viability. Stillbirth and early childhood death may occur in families with more severe bi-allelic *GOT2* mutations, as also suggested by the homozygous Got2-knockout mice which were not viable and by the embryonic death which was observed in the zebrafish model. GOT2-deficient individuals share a phenotype of epilepsy, intellectual disability, and several biochemical features with persons suffering from other MAS defects (*MDH2*, *SLC25A12*, *SLC25A13*).[9,33,34] GOT2 deficiency clinically also resembles the three known inborn errors of serine metabolism (genes involved: *PHGDH*, *PSAT1*, *PSPH* [MIM: 606879, 610936, 172480]) with microcephaly, intellectual developmental disorder, and epilepsy. GOT2 deficiency should be considered in the differential diagnosis of epileptic encephalopathy especially in the presence of high lactate, increased ammonia and citrulline, and decreased serine. Theoretically other MAS defects may also lead to secondary decreased serine synthesis due to cytosolic redox imbalance but low serine levels have not yet been reported in such case subjects.

Western blot and enzyme activity data show that the *GOT2* mutations in our affected individuals prevent GOT2 expression or render the GOT2-protein unstable. GOT2 deficiency impacts the malate-aspartate shuttle

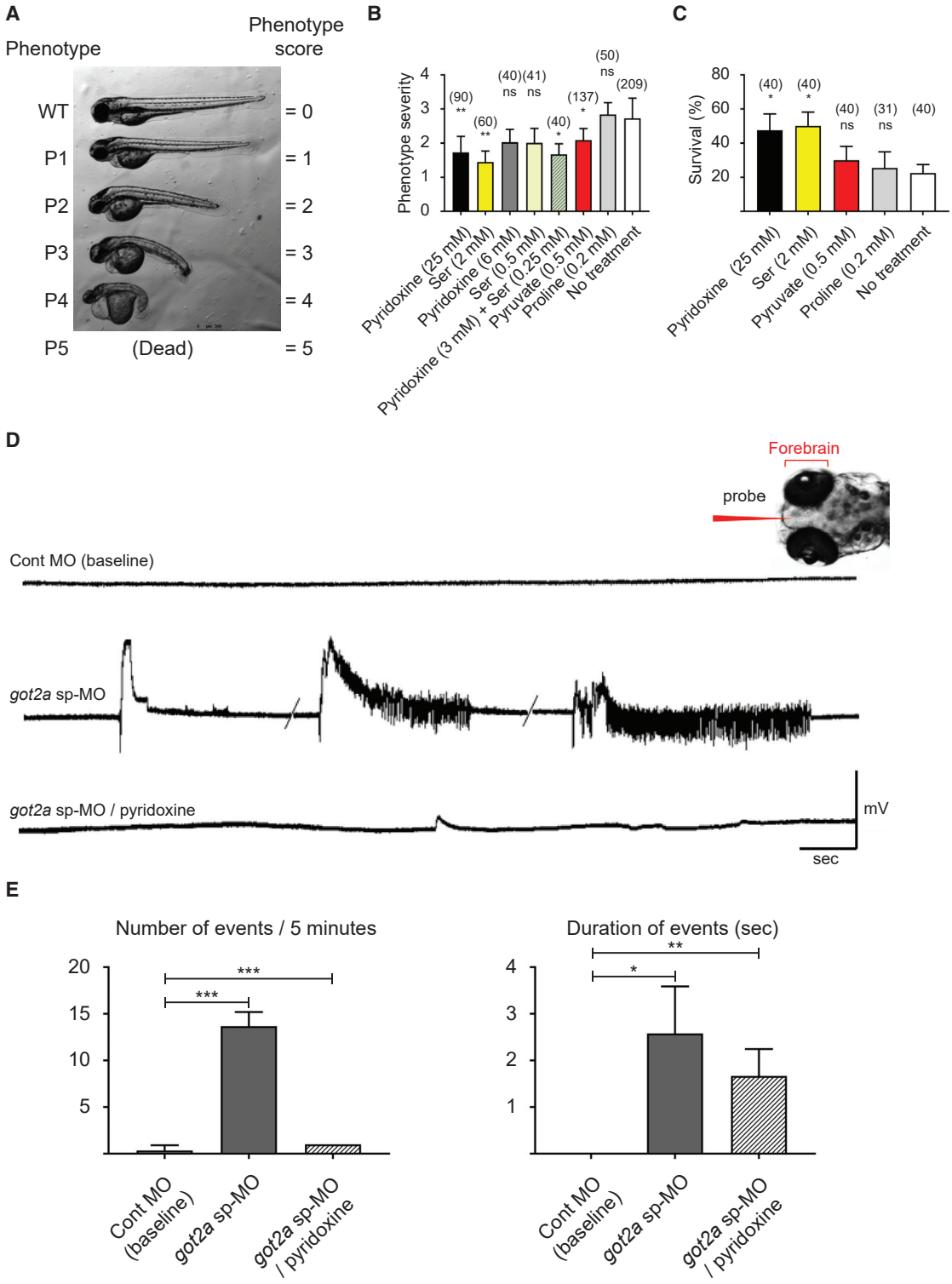

Figure 5. Knockdown of *got2a* in Zebrafish Perturbs Brain and Embryonic Development and Function, which Can Be Rescued by Pyridoxine and Serine

(A) Phenotype severity and rescue scoring system for *got2a* knockdown embryos. Bright field images of 3 day post fertilization (dpf) WT embryos injected with control morpholino (Cont MO) and/or got2a ATG blocking morpholino (got2a MO). The *got2a* morphants were scored in five different categories (P1 to P5) based on the phenotype severities.

(B) Pyridoxine, serine, and pyruvate decrease got2a morphant's phenotype severity. Number of larvae per condition were shown in parentheses. 2 nL of morpholino (0.4 mM working solution) was injected. Compounds were added at 6 h post-fertilization (hpf) in 24-well plates. Every 24 h, dead embryos were removed and the compounds were replaced with fresh solution. Phenotype was characterized at 3 dpf. For phenotype severity calculation, the following "phenotype scores" were used: P0, normal: 0; P1, small brain, enlarged yolk, and mild cardiac edema: 1; P2, smaller brain, enlarged yolk, mild cardiac edema, and shortened body: 2; P3, smaller brain, enlarged

(legend continued on next page)

and subsequently the overall cellular NADH/NAD^+ ratio with consequences for NAD-dependent enzymes and pathways. Elevated blood lactate concentrations of the affected individuals can be explained as direct consequence of the impaired re-oxidation of cytosolic NADH due to the defective MAS. Interestingly, hyperlactatemia is also present in MDH2 deficiency, another disorder impairing the MAS (Figure 1).[9]

All four affected individuals had a mild but persistent hyperammonemia, with individual 1 also having mild hypercitrullinemia. Both can be explained by a secondary urea cycle defect in GOT2 deficiency. In humans, the amount of aspartate taken up from the blood is very low,[35] rendering cells highly dependent on their mitochondrial aspartate production. In GOT2 deficiency, the intramitochondrial synthesis of aspartate from oxaloacetate is decreased, leading to lower concentrations of aspartate in the mitochondrion and the cytosol. In one of the cytoplasmic steps of the urea cycle in liver, the enzyme argininosuccinate synthetase requires aspartate as a substrate. Aspartate shortage leads to reduced argininosuccinate synthesis, and to citrulline accumulation, with hyperammonemia as a final consequence of diminished urea cycle activity.[6]

A further striking observation in individual 1 was a consistently reduced plasma serine concentration in the same range as observed in individuals with serine biosynthesis defects. No mutations were found in genes implicated in the biosynthesis of serine. Stable isotope-labeling studies showed decreased serine synthesis from $^{13}C_6$-glucose in fibroblasts of affected individuals and in GOT2-knockout HEK293 cells. Intracellular serine can originate from four sources: (1) the diet, (2) *de novo* biosynthesis, (3) glycine, or (4) protein and phospholipid degradation.[36] The first reaction in *de novo* serine biosynthesis is catalyzed by the NAD^+-dependent enzyme 3-phosphoglycerate dehydrogenase. The low serine and glycine production observed in GOT2 deficiency is most likely due to an increased NADH/NAD^+ ratio as a consequence of a dysfunctional MAS. Pyridoxine is essential for serine *de novo* biosynthesis,[37] so we cannot exclude that the mechanism of pyridoxine responsiveness may be partly due to a direct effect on boosting serine synthesis by a mechanism other than restoring the NADH/NAD^+ redox balance.

To investigate whether correction of the cytosolic NADH/NAD^+ ratio could restore serine and glycine *de novo* synthesis, we supplemented the culture medium of GOT2-deficient HEK293 cells with glycerol or pyruvate. The rationale behind glycerol addition was to stimulate the activity of the glycerol 3-phosphate shuttle, a second system for the regeneration of NAD^+ from NADH. No effect of glycerol on serine and glycine synthesis was observed, suggesting that the MAS is the predominant NAD(H) redox shuttle, at least in HEK293 cells. After incubating with pyruvate, which is enzymatically reduced to lactate in the cytosol while re-oxidizing NADH to NAD^+, complete normalization of serine and glycine synthesis was observed, supporting our hypothesis that serine biosynthesis is hampered by the impaired cytosolic redox imbalance. GOT2 deficiency is a mitochondriopathy with metabolic consequences in mitochondria and in the cytoplasm due to redox imbalance. Our data explain the mitochondrial pathomechanism and clarify how GOT2 deficiency impacts serine biosynthesis and possibly other NAD(H)-dependent reactions and how the affected individuals benefit from serine and/or pyridoxine supplementation.

Individual 1 was free of seizures only when a combination of serine and pyridoxine was administered. PLP is an obligatory co-activator for all transaminases, including GOT2. It may stimulate residual GOT2 activity possibly by improving the proper folding of GOT2.

Interestingly, the only other individual with uncontrolled seizures (individual 4) was put on pyridoxine-only therapy for 8 months. His epilepsy was better controlled and his cognitive functions and alertness improved. Once serine supplementation was added to the treatment regimen, his seizures were fully controlled with better cognition and improved physical activity. In a period that serine was unavailable, the seizures returned and disappeared again when serine was reintroduced. Treatment could not be started in individuals 2 and 3.

Theoretically, pyruvate supplementation might be considered as treatment strategy. Re-oxidation of cytosolic NADH by pyruvate supplementation *in vitro* led to full

yolk, severe cardiac edema, and curved body: 3; P4, very small brain, enlarged yolk, very severe cardiac edema, deformed tail, and round body shape: 4; P5, dead: 5. Average phenotype severity = $\sum$ n x (Phenotype score) / N. n, number of embryos showing a specific phenotype in a well; N, total initial number of embryos in a well. Treated samples were compared to non-treated conditions using one-way ANOVA test (*$p < 0.05$; **$p < 0.01$; ns, not significant).

(C) Pyridoxine and serine increase the survival of *got2a* morphants at 2 dpf. Number of larvae per condition is shown in parentheses. 4 nL of morpholino (0.8 mM working solution) was injected. Compounds were added at 6 h post-fertilization (hpf) in 24-well plates. Every 24 h, dead embryos were removed and the compounds were replaced with fresh solution. The ratio of alive to total number of larvae was counted and survival percentage calculated at 2 dpf (a dead zebrafish embryo defined as having no heartbeat and no response to stimuli). Treated samples were compared to non-treated conditions using one-way ANOVA test (*$p < 0.05$; ns, not significant).

(D) *got2a* knockdown provoked seizure-like EEG spikes in the forebrain that are rescued by treatment with pyridoxine in 48 hpf embryos. Newly fertilized zebrafish embryos are injected with control morpholino (Cont MO) or *got2a* splicing morpholino (sp-MO). Embryos injected with *got2a* sp-MO showed EEG spike discharges, not present in traces from embryos injected with Cont MO.

(E) Analysis of EEG traces. Number of events in 5 min recordings and the duration of each event in seconds (sec) in embryos injected with Cont MO, *got2a* sp-MO, and *got2a* sp-MO and treated with pyridoxine. Each event corresponds to a single spike discharge. Bars represent the mean ± SEM. N = 3 embryos per treatment. *$p < 0.05$ and ***$p < 0.001$.

correction of serine biosynthesis in GOT2-deficient cells. This effect is explained by the pyruvate-induced correction of the high NADH/NAD^+ ratio in the cytosol. Interestingly, administration of sodium pyruvate with L-arginine proved effective in treating a person with a defect in *SCL25A13*.[38] Increased lactate formation from pyruvate may form an unwanted side-effect of this approach. Defects in the MAS-system only affect the oxidation of cytosolic NADH and not of intramitochondrial NADH, which implies that the best therapy strategy would be to provide substrates that do not produce NADH in the cytosol, e.g., fatty acids especially medium chain triglycerides. For GOT2-deficient individuals, we suggest a diet low in carbohydrates, high in fat, and supplemented with ketone bodies that circumvents the issue of acidification due to lactate production. Our zebrafish modeling of GOT2 deficiency demonstrated that serine and pyridoxine treatment would likely deliver a synergetic effect. These could be further explored as therapeutic strategies in disease management.

Future research on this MAS defect should focus on the identification of more affected individuals, characterization of the full phenotypic and genotypic spectrum, identification of biomarkers and other treatment targets, as well as implementation and evaluation of therapeutic interventions in more case subjects.

Supplemental Data

Supplemental Data can be found online at https://doi.org/10.1016/j.ajhg.2019.07.015.

Acknowledgments

We are grateful to the affected individuals and their families for their participation in this study. We acknowledge the clinicians and laboratory scientists involved in the management of these individuals and for providing their medical reports. We acknowledge the following individuals for their contributions: Jessica Lee, Marion Ybema-Antoine, and Frans van den Brandt for excellent technical support; Ms. Xiaohua Han for Sanger sequencing; Ms. Dora Pak and Ms. Evelyn Lomba for research management support; Ms. Michelle Higginson for DNA extraction, sample handling, and technical data; Ms. Lauren Muttumacoroe and Ms. Aisha Ghani for data management; and Dr. Tom J. de Koning, UMCG Groningen, for advice on serine supplementation.

Funding to C.D.M.v.K. was provided by the Canadian Institutes of Health Research (grant number #301221), Rare Diseases Foundation (microgrant 1788), National Ataxia Foundation, and Canadian Rare Diseases Model Organisms and Mechanisms Network. Informatics infrastructure supported by Genome British Columbia and Genome Canada (ABC4DE Project). C..D.M.v.K. is a recipient of the Michael Smith Foundation for Health Foundation Research Scholar Award and a Foundation Metakids salary award. R.v.d.L. and W.W.W. were supported by a Rubicon fellowship from the Netherlands Organization for Scientific Research (NWO and ZONMW, 40-45200-98-015, to R.v.d.L.), Genome Canada (255ONT), and Canadian Institutes of Health Research (CIHR; BOP-149430). X.-Y.W. was funded by Engineering Research Council of Canada (NSERC) (RGPIN 05389-14), Brain Canada Foundation (PSG14-3505), and Canada Foundation for Innovation (CFI #26233). This work was supported by Foundation Metakids (2013-046 to J.J.J. and N.M.V.-D.), NIH R01NS098004, NS048453, QNRF NPRP6-1463, the Simons Foundation Autism Research Initiative 275275, the Rady Children's Institute for Genomic Medicine, and Howard Hughes Medical Institute (to J.G.G.), and by the E.C. Noyons foundation (to R.A.W.). We thank the Broad Institute (UM1HG008900 to D. MacArthur) and the Yale Center for Mendelian Disorders (U54HG006504 to R. Lifton and M. Gunel).

Declaration of Interests

The authors declare no competing interests.

Received: March 29, 2019
Accepted: July 22, 2019
Published: August 15, 2019

Web Resources

GenBank, https://www.ncbi.nlm.nih.gov/genbank/
OMIM, https://www.omim.org/
RCSB Protein Data Bank, http://www.rcsb.org/pdb/home/home.do
UCSC Genome Browser, https://genome.ucsc.edu
YASARA, http://www.yasara.org

References

1. Lu, M., Zhou, L., Stanley, W.C., Cabrera, M.E., Saidel, G.M., and Yu, X. (2008). Role of the malate-aspartate shuttle on the metabolic response to myocardial ischemia. J. Theor. Biol. *254*, 466–475.
2. Williamson, D.H., Lund, P., and Krebs, H.A. (1967). The redox state of free nicotinamide-adenine dinucleotide in the cytoplasm and mitochondria of rat liver. Biochem. J. *103*, 514–527.
3. Dawson, A.G. (1979). Oxidation of cytosolic NADH formed during aerobic metabolism in mammalian cells. Trends Biochem. Sci. *4*, 171–176.
4. Purvis, J.L., and Lowenstein, J.M. (1961). The relation between intra- and extramitochondrial pyridine nucleotides. J. Biol. Chem. *236*, 2794–2803.
5. Wibom, R., Lasorsa, F.M., Töhönen, V., Barbaro, M., Sterky, F.H., Kucinski, T., Naess, K., Jonsson, M., Pierri, C.L., Palmieri, F., and Wedell, A. (2009). AGC1 deficiency associated with global cerebral hypomyelination. N. Engl. J. Med. *361*, 489–495.
6. Saheki, T., and Kobayashi, K. (2002). Mitochondrial aspartate glutamate carrier (citrin) deficiency as the cause of adult-onset type II citrullinemia (CTLN2) and idiopathic neonatal hepatitis (NICCD). J. Hum. Genet. *47*, 333–341.
7. Fiermonte, G., Parisi, G., Martinelli, D., De Leonardis, F., Torre, G., Pierri, C.L., Saccari, A., Lasorsa, F.M., Vozza, A., Palmieri, F., and Dionisi-Vici, C. (2011). A new Caucasian case of neonatal intrahepatic cholestasis caused by citrin deficiency (NICCD): a clinical, molecular, and functional study. Mol. Genet. Metab. *104*, 501–506.
8. Hayasaka, K., Numakura, C., Toyota, K., Kakizaki, S., Watanabe, H., Haga, H., Takahashi, H., Takahashi, Y., Kaneko, M., Yamakawa, M., et al. (2014). Medium-chain triglyceride supplementation under a low-carbohydrate formula is a promising therapy for adult-onset type II citrullinemia. Mol. Genet. Metab. Rep. *1*, 42–50.

9. Ait-El-Mkadem, S., Dayem-Quere, M., Gusic, M., Chaussenot, A., Bannwarth, S., François, B., Genin, E.C., Fragaki, K., Volker-Touw, C.L.M., Vasnier, C., et al. (2017). Mutations in MDH2, Encoding a Krebs Cycle Enzyme, Cause Early-Onset Severe Encephalopathy. Am. J. Hum. Genet. *100*, 151–159.
10. Langmead, B., and Salzberg, S.L. (2012). Fast gapped-read alignment with Bowtie 2. Nat. Methods *9*, 357–359.
11. Tarailo-Graovac, M., Shyr, C., Ross, C.J., Horvath, G.A., Salvarinova, R., Ye, X.C., Zhang, L.-H., Bhavsar, A.P., Lee, J.J.Y., Drögemöller, B.I., et al. (2016). Exome Sequencing and the Management of Neurometabolic Disorders. N. Engl. J. Med. *374*, 2246–2255.
12. Cingolani, P., Platts, A., Wang, L., Coon, M., Nguyen, T., Wang, L., Land, S.J., Lu, X., and Ruden, D.M. (2012). A program for annotating and predicting the effects of single nucleotide polymorphisms, SnpEff: SNPs in the genome of Drosophila melanogaster strain w1118; iso-2; iso-3. Fly (Austin) *6*, 80–92.
13. Jay, J.J., and Brouwer, C. (2016). Lollipops in the Clinic: Information Dense Mutation Plots for Precision Medicine. PLoS ONE *11*, e0160519.
14. Katoh, K., and Standley, D.M. (2013). MAFFT multiple sequence alignment software version 7: improvements in performance and usability. Mol. Biol. Evol. *30*, 772–780.
15. Waterhouse, A.M., Procter, J.B., Martin, D.M., Clamp, M., and Barton, G.J. (2009). Jalview Version 2–a multiple sequence alignment editor and analysis workbench. Bioinformatics *25*, 1189–1191.
16. Jiang, X., Wang, J., Chang, H., and Zhou, Y. (2016). Recombinant expression, purification and crystallographic studies of the mature form of human mitochondrial aspartate aminotransferase. Biosci. Trends *10*, 79–84.
17. Han, Q., Robinson, H., Cai, T., Tagle, D.A., and Li, J. (2011). Biochemical and structural characterization of mouse mitochondrial aspartate aminotransferase, a newly identified kynurenine aminotransferase-IV. Biosci. Rep. *31*, 323–332.
18. Bordoli, L., Kiefer, F., Arnold, K., Benkert, P., Battey, J., and Schwede, T. (2009). Protein structure homology modeling using SWISS-MODEL workspace. Nat. Protoc. *4*, 1–13.
19. Ran, F.A., Hsu, P.D., Wright, J., Agarwala, V., Scott, D.A., and Zhang, F. (2013). Genome engineering using the CRISPR-Cas9 system. Nat. Protoc. *8*, 2281–2308.
20. Renkema, G.H., Wortmann, S.B., Smeets, R.J., Venselaar, H., Antoine, M., Visser, G., Ben-Omran, T., van den Heuvel, L.P., Timmers, H.J.L.M., Smeitink, J.A., and Rodenburg, R.J.T. (2015). SDHA mutations causing a multisystem mitochondrial disease: novel mutations and genetic overlap with hereditary tumors. Eur. J. Hum. Genet. *23*, 202–209.
21. Prinsen, H.C.M.T., Schiebergen-Bronkhorst, B.G.M., Roeleveld, M.W., Jans, J.J.M., de Sain-van der Velden, M.G.M., Visser, G., van Hasselt, P.M., and Verhoeven-Duif, N.M. (2016). Rapid quantification of underivatized amino acids in plasma by hydrophilic interaction liquid chromatography (HILIC) coupled with tandem mass-spectrometry. J. Inherit. Metab. Dis. *39*, 651–660.
22. Baraban, S.C. (2013). Forebrain electrophysiological recording in larval zebrafish. J. Vis. Exp. *71*, 2–5.
23. Zabinyakov, N., Bullivant, G., Cao, F., Fernandez Ojeda, M., Jia, Z.P., Wen, X.-Y., Dowling, J.J., Salomons, G.S., and Mercimek-Andrews, S. (2017). Characterization of the first knockout aldh7a1 zebrafish model for pyridoxine-dependent epilepsy using CRISPR-Cas9 technology. PLoS ONE *12*, e0186645.
24. Kircher, M., Witten, D.M., Jain, P., O'Roak, B.J., Cooper, G.M., and Shendure, J. (2014). A general framework for estimating the relative pathogenicity of human genetic variants. Nat. Genet. *46*, 310–315.
25. Choi, Y., and Chan, A.P. (2015). PROVEAN web server: a tool to predict the functional effect of amino acid substitutions and indels. Bioinformatics *31*, 2745–2747.
26. Adzhubei, I., Jordan, D.M., and Sunyaev, S.R. (2013). Predicting functional effect of human missense mutations using PolyPhen-2. Curr. Protoc. Hum. Genet. *Chapter 7*, 20.
27. Kumar, P., Henikoff, S., and Ng, P.C. (2009). Predicting the effects of coding non-synonymous variants on protein function using the SIFT algorithm. Nat. Protoc. *4*, 1073–1081.
28. van Karnebeek, C.D.M., Bonafé, L., Wen, X.-Y., Tarailo-Graovac, M., Balzano, S., Royer-Bertrand, B., Ashikov, A., Garavelli, L., Mammi, I., Turolla, L., et al. (2016). NANS-mediated synthesis of sialic acid is required for brain and skeletal development. Nat. Genet. *48*, 777–784.
29. Wen, X.-Y., Tarailo-Graovac, M., Brand-Arzamendi, K., Willems, A., Rakic, B., Huijben, K., Da Silva, A., Pan, X., El-Rass, S., Ng, R., et al. (2018). Sialic acid catabolism by N-acetylneuraminate pyruvate lyase is essential for muscle function. JCI Insight *3*, 1–20.
30. Rahman, J., and Rahman, S. (2018). Mitochondrial medicine in the omics era. Lancet *391*, 2560–2574.
31. Sharma, S., and Prasad, A.N. (2017). Inborn errors of metabolism and epilepsy: Current understanding, diagnosis, and treatment approaches. Int. J. Mol. Sci. *18*, 18.
32. Pena, I.A., MacKenzie, A., and Van Karnebeek, C.D.M. (2017). Current knowledge for pyridoxine-dependent epilepsy: a 2016 update. Expert Rev. Endocrinol. Metab. *12*, 5–20.
33. Kobayashi, K., Sinasac, D.S., Iijima, M., Boright, A.P., Begum, L., Lee, J.R., Yasuda, T., Ikeda, S., Hirano, R., Terazono, H., et al. (1999). The gene mutated in adult-onset type II citrullinaemia encodes a putative mitochondrial carrier protein. Nat. Genet. *22*, 159–163.
34. Dahlin, M., Martin, D.A., Hedlund, Z., Jonsson, M., von Döbeln, U., and Wedell, A. (2015). The ketogenic diet compensates for AGC1 deficiency and improves myelination. Epilepsia *56*, e176–e181.
35. Palmieri, F. (2004). The mitochondrial transporter family (SLC25): physiological and pathological implications. Pflugers Arch. *447*, 689–709.
36. de Koning, T.J., Snell, K., Duran, M., Berger, R., Poll-The, B.-T., and Surtees, R. (2003). L-serine in disease and development. Biochem. J. *371*, 653–661.
37. Ramos, R.J., Pras-Raves, M.L., Gerrits, J., van der Ham, M., Willemsen, M., Prinsen, H., Burgering, B., Jans, J.J., and Verhoeven-Duif, N.M. (2017). Vitamin B6 is essential for serine de novo biosynthesis. J. Inherit. Metab. Dis. *40*, 883–891.
38. Mutoh, K., Kurokawa, K., Kobayashi, K., and Saheki, T. (2008). Treatment of a citrin-deficient patient at the early stage of adult-onset type II citrullinaemia with arginine and sodium pyruvate. J. Inherit. Metab. Dis. *31* (*Suppl 2*), S343–S347.